SCIENCE CHINA
Information Sciences

• Supplementary File •

# Performance-Guaranteed Finite-Time Exact-Tracking of Strict-Feedback Systems with Actuator Faults

Yuzhi KONG[1,2], Xiaoqun WU[1*], Bing MAO[1], Jianwen FENG[3] & Tingwen HUANG[4]

[1] *College of Computer Science and Software Engineering, Shenzhen University, Shenzhen 518060, China*
[2] *School of Mathematics and Statistics, Wuhan University, Wuhan 430072, China*
[3] *School of Mathematical Sciences, Shenzhen University, Shenzhen 518060, China*
[4] *Faculty of Computer Science and Control Engineering, Shenzhen University of Advanced Technology, Shenzhen 518055, China*

## Appendix A Control design and stability analysis

To complete the controll design, we introduce the following assumptions and notation.

**Assumption 1.** The reference signal $y_0(t)$ and its derivative $\dot{y}_0(t)$ are bounded, continuous. Only $y_0(t)$ is available for the controller design.

**Assumption 2.** The external disturbance $d_i(t)$ is piecewise continuous in $t$ and there exists an unknown constant $d_i^0 > 0$ such that $|d_i(t)| \leqslant d_i^0$, $(i = 1, 2, \ldots, n)$.

**Assumption 3.** There exist unknown constants $\tau_f > 0$ and $\bar{\theta} > 0$ such that $\tau_f \leqslant \tau(t) \leqslant 1$ and $|\theta(t)| \leqslant \bar{\theta}$.

**Assumption 4.** There exists a positive and continuous function $L_i(\bar{\boldsymbol{x}}_i(t), \bar{\boldsymbol{y}}_i(t), t)$ such that for any $\bar{\boldsymbol{x}}_i \in R^i$ and $\bar{\boldsymbol{y}}_i \in R^i$, $|f_i(\bar{\boldsymbol{x}}_i(t)) - f_i(\bar{\boldsymbol{y}}_i(t))| \leqslant L_i(\bar{\boldsymbol{x}}_i(t), \bar{\boldsymbol{y}}_i(t), t)\|\bar{\boldsymbol{x}}_i(t) - \bar{\boldsymbol{y}}_i(t)\|$ holds for $i = 2, 3, \ldots, n$, where $L_i(\bar{\boldsymbol{x}}_i(t), \bar{\boldsymbol{y}}_i(t), t)$ is bounded if $\bar{\boldsymbol{x}}_i(t)$ and $\bar{\boldsymbol{y}}_i(t)$ are bounded.

**Assumption 5.** Without loss of generality, the sign of function $g_i(\bar{\boldsymbol{x}}_i(t))$ is definite. Suppose that there exist unknown positive constants $\underline{g}_i$ and $\bar{g}_i$ such that $\underline{g}_i \leqslant g_i(\bar{\boldsymbol{x}}_i(t)) \leqslant \bar{g}_i$.

**Assumption 6.** The sign of function $g_i(\bar{\boldsymbol{x}}_i(t))$ is unknown for $i = 1, 2, \ldots, n-1$, and for simplicity, the sign of $g_n(\bar{\boldsymbol{x}}_n(t))$ is known and assumed to be positive. Without loss of generality, suppose that there exist unknown constants $\underline{g}_i > 0$ and $\bar{g}_i > 0$ such that $\underline{g}_i \leqslant |g_i(\bar{\boldsymbol{x}}_i(t))| \leqslant \bar{g}_i$.

**Remark 1.** Assumption 1 is standard in the literature [1–3]. It is commonly employed to ensure tracking control for the class of systems under consideration, as evidenced by [4, 5]. Similarly, Assumption 2 is also conventional and widely adopted to guarantee tracking performance, as can be found in [6–8]. In Assumption 3, the loss of effectiveness $\tau(t)$ is lower bounded by an unknown positive constants $\tau_f$. This makes the entire system controllable, and $\tau_f$ only shows up in the stability analysis. Assumption 4 can be regarded as a generalized Lipschitz condition imposed on unknown nonlinear terms. It should be emphasized in Assumptions 5 and 6 that both the lower and upper bounds of $g_i(\bar{\boldsymbol{x}}_i(t))$, where $i = 1, 2, \ldots, n$, are unknown. This is less restrictive than the assumption in [9], which require the knowledge of all upper and lower bounds of unknown control coefficients. In real-world control scenarios, it can be difficult to obtain the bound of a practical system.

**Notation**. Throughout this Appendix, $R^n$ denotes the $n$-dimensional Euclidean space. $|x|$ denotes the absolute value of scalar $x$. $||\boldsymbol{x}||$ denotes the Euclidean norm of vector $\boldsymbol{x}$. $\boldsymbol{x}^\top$ represents the transpose of vector $\boldsymbol{x}$, respectively. For a function $V$ that is continuous but non-differentiable at $\omega_0$, the right Dini upper derivative at $\omega_0$ is defined as: $D^+V(\omega_0) = \limsup_{h\to 0^+} \frac{V(\omega_0+h)-V(\omega_0)}{h}$. For simplicity, the variable $t$ is omitted without causing ambiguity in what follows.

### Appendix A.1 Control design of Theorem 1

In this subsection, we will first establish the control design for the system with known control directions under Assumptions 1-5. Then, we will consider the case where only the direction of actual controller $g_n(\bar{\boldsymbol{x}}_n)$ is known. In order to achieve the control objectives, virtual signals and an actual controller are proposed. For clarity and the reader's convenience, we begin by reiterating the definition of the function originally introduced in the letter: First, the following exponential function $\rho_i(t)$:

$$\rho_i(t) = \left(\frac{\pi}{2} - \rho_{i\infty}\right) \mathrm{e}^{-\rho_{i1} t} + \rho_{i\infty},\ i = 1, 2, \ldots, n, \tag{A1}$$

where $\frac{\pi}{2} > \rho_{i\infty} > 0$ and $\rho_{i1} > 0$. In this case, $\rho_i(0) = \frac{\pi}{2}$, $\dot{\rho}_i(t) < 0$ and $\dot{\rho}_i(t)$ is bounded. Then, the tracking error $e_1(t)$:

$$e_1(t) = y(t) - y_0(t), \tag{A2}$$

* Corresponding author (email: xqwu@whu.edu.cn)

$$e_i(t) = x_i(t) - \alpha_{i-1}(t),\ i = 2, 3, \dots, n, \tag{A3}$$

and the virtual control signals $\beta_{i-1}(t)$, the output $\alpha_i(t)$ and error $z_i(t)$ of the first-order filter on $\beta_{i-1}(t)$:

$$\bar{d}_i \dot{\alpha}_i(t) + \alpha_i(t) = \beta_i(t),\ \alpha_i(0) = \beta_i(0),\ i = 1, 2, \dots, n-1, \tag{A4}$$

$$z_i(t) = \beta_i(t) - \alpha_i(t),\ i = 1, 2, \dots, n-1, \tag{A5}$$

where $\bar{d}_i > 0$. Then, the transformed errors $\omega_i(t)$ and $k_i(t)$:

$$\omega_i(t) = \tan\left(\frac{\pi}{2} k_i(t)\right),\ i = 1, 2, \dots, n, \tag{A6}$$

$$k_i(t) = \frac{\arctan(e_i(t))}{\rho_i(t)},\ i = 1, 2, \dots, n. \tag{A7}$$

Additionally, the integral sliding mode variables as:

$$s_i(t) = \omega_i(t) + \lambda_i \int_0^t \mathrm{sign}(\omega_i(\mu))\mathrm{d}\mu,\ i = 1, 2, \dots, n, \tag{A8}$$

and low-pass filters as:

$$\bar{\tau}_i \dot{\zeta}_i(t) + \zeta_i(t) = -\mathrm{sign}(s_i(t)),\ \zeta_i(0) = 0,\ i = 1, 2, \dots, n, \tag{A9}$$

where $\lambda_i, \bar{\tau}_i > 0$ are a positive constant and the filter constant, respectively. The virtual signals $\beta_i$ and actual controller $v$ of known control directions:

$$\beta_1 = -c_1 \mathrm{sign}(\xi_1), \tag{A10}$$

$$\beta_i = -\frac{c_i \sqrt{s_i + \varrho_i |s_i|}}{\xi_i} - \varrho_i' \xi_i \phi_i \left(\bar{L}_i^2 + \frac{z_{i-1}^2}{\bar{d}_{i-1}^2}\right) - \frac{|\xi_{i-1}|\phi_{i-1}(z_{i-1}^2 + x_i^2)}{\xi_i \phi_i},\ i = 2, 3, \dots, n-1, \tag{A11}$$

$$v = -\frac{1}{\gamma_n}\left(\frac{c_n \sqrt{s_n + \varrho_n |s_n|}}{\xi_n} + \varrho_n' \xi_n \phi_n \left(\bar{L}_n^2 + \frac{z_{n-1}^2}{\bar{d}_{n-1}^2}\right) + \frac{|\xi_{n-1}|\phi_{n-1}(z_{n-1}^2 + x_n^2)}{\xi_n \phi_n} + \sum_{i=1}^{n} \frac{|\xi_i|\phi_i H_i}{\xi_n \phi_n}\right), \tag{A12}$$

where $c_i > 0$ $(i = 1, 2, \dots, n)$, $\varrho_i > 1$, and $\varrho_i' > 0$ $(i = 2, 3, \dots, n)$ are scalars to be designed. Additionally, we define $\bar{L}_i = L_i(\bar{\boldsymbol{x}}_i, \bar{\boldsymbol{y}}_i, t)\|\bar{\boldsymbol{x}}_i - \bar{\boldsymbol{y}}_i\|$, and $\xi_1 = s_1$, $\xi_i = 1 + \varrho_i \mathrm{sign}(s_i)$ $(i = 2, 3, \dots, n)$. Under these definitions, it follows that $\xi_i \neq 0$ for all $s_i$ where $i = 2, 3, \dots, n$. Let $s(t) = \max\{|s_i(t)|, \dots, |s_n(t)|\}$. Then the feedback gain $H_i(t)$ is defined as:

$$H_i(t) = h_i(t) + r_i(\|\omega\|_t + |Q_t|)\mathrm{e}^{-\bar{r}_i t}, \tag{A13}$$

where $\|\omega\|_t = \max\{\sup_{0 \leqslant \mu \leqslant t} |\omega_1(\mu)|, \dots, \sup_{0 \leqslant \mu \leqslant t} |\omega_n(\mu)|\}$, $r_i$, $\bar{r}_i > 0$, $Q_t = \{q \in N^+ | s(t_q) = 0, \mathrm{sign}(s(t_q^-)) \neq 0, t_{q-1} < t_q \leqslant t, t_0 = 0\}$, $N^+$ represents the positive integer set, and $|Q_t|$ is the cardinality of $Q_t$. Then the switching gain $h_i(t)$ is designed as follows:

- if $s(t) \neq 0$, then $h_i(t)$ evolves according to

$$\dot{h}_i(t) = \bar{h}_{i1}|s_i(t)| + \bar{h}_{i2}, h_i(0) > 0; \tag{A14}$$

- if $s(t) = 0$, then $h_i(t)$ is switched to

$$h_i(t) = \bar{h}_{i3}|\zeta_i(t)| + \bar{h}_{i4}, \tag{A15}$$

where $\bar{h}_{ij} > 0$, $j = 1, 2, 4$ and $\bar{h}_{i3} = H_i(\underline{t}_i)$, with $\underline{t}_i$ being the latest instant up to $t$ such that $\mathrm{sign}(s(\underline{t}_i^-)) \neq 0$ and $s(\underline{t}_i) = 0$.

According to Eq. (A7), $e_i = \tan(k_i \rho_i)$. Taking the derivative of $e_1$, and combining it with Eq. (A2), we have $\dot{e}_1 = \frac{1}{\cos^2(k_1 \rho_1)}(\dot{k}_1 \rho_1 + k_1 \dot{\rho}_1) = g_1(\bar{\boldsymbol{x}}_1)x_2 + f_1(\bar{\boldsymbol{x}}_1) + d_1 - \dot{y}_0$. Therefore, we get

$$\begin{aligned}\dot{k}_1 =& \frac{1}{\rho_1}[\gamma_1(g_1(\bar{\boldsymbol{x}}_1)x_2 + f_1(\bar{\boldsymbol{x}}_1) + d_1 - \dot{y}_0) - k_1 \dot{\rho}_1] \\ =& \frac{1}{\rho_1}[\gamma_1 g_1(\bar{\boldsymbol{x}}_1)(\tan(k_2 \rho_2) + \beta_1 - z_1) + \gamma_1(f_1(\bar{\boldsymbol{x}}_1) + d_1 - \dot{y}_0) - k_1 \dot{\rho}_1] \\ \triangleq& \Gamma_1(k_1, k_2, t).\end{aligned} \tag{A16}$$

Similarly, we have

$$\begin{aligned}\dot{k}_i =& \frac{1}{\rho_i}[\gamma_i\left(g_i(\bar{\boldsymbol{x}}_i)x_{i+1} + f_i(\bar{\boldsymbol{x}}_i) + d_i - \frac{z_{i-1}}{\bar{d}_{i-1}}\right) - k_i \dot{\rho}_i] \\ \triangleq& \Gamma_i(k_1, \dots, k_{i+1}, t),\ i = 2, 3, \dots, n-1,\end{aligned} \tag{A17}$$

$$\begin{aligned}\dot{k}_n =&\frac{1}{\rho_n}[\gamma_n\left(g_n(\bar{\boldsymbol{x}}_n)u+f_n(\bar{\boldsymbol{x}}_n)+d_n-\frac{z_{n-1}}{\bar{d}_{n-1}}\right)-k_n\dot{\rho}_n]\\ \triangleq&\Gamma_n(k_1,\dots,k_n,t),\end{aligned}\tag{A18}$$

where $0<\gamma_i=\cos^2(k_i\rho_i)\leqslant 1$, $(i=1,2,\dots,n)$. Let $\boldsymbol{k}=[k_1,\dots,k_n]^\top\in R^n,\Gamma=[\Gamma_1,\dots,\Gamma_n]^\top\in R^n,\Xi\triangleq\underbrace{(-1,1)\times\cdots\times(-1,1)}_{n}$.

Combining Eqs. (A16)-(A18), we have

$$\dot{\boldsymbol{k}}=\Gamma(\boldsymbol{k},t).$$

We can obtain that $\Gamma(\boldsymbol{k},t)$ is locally Lipschitz in $\boldsymbol{k}$ since $\rho_i$, $\dot{\rho}_i$, $g_i(\bar{\boldsymbol{x}}_i)$, $\gamma_i$ are bounded. From Eqs. (A1) and (A6), we have $\boldsymbol{k}(0)\in\Xi$. From Assumption 2, and Eqs. (A10)-(A12), we can get that $d_i$, $\beta_i$, $z_i$, $v$, $g_i(\bar{\boldsymbol{x}}_i)$ are piecewise continuous and $f_i(\bar{\boldsymbol{x}}_i)$, $y_0$, $\dot{y}_0$, $\rho_i$, $\dot{\rho}_i$ are continuous. Thus, $\Gamma(\boldsymbol{k},t)$ is piecewise continuous in $t$. Consequently, according to Lemma 1 of [10], there exists a unique maximal solution $\boldsymbol{k}\in\Xi$ on $[0,t_{\max})$, where $0<t_{\max}\leqslant+\infty$.

Then, from Eq. (A6), we have $\dot{\omega}_i=\frac{\pi}{2\cos^2(\frac{\pi}{2}k_i)}\dot{k}_i$. Let $\phi_i=\frac{\pi}{2\rho_i\cos^2(\frac{\pi}{2}k_i)}$, $(i=1,2,\dots,n)$. From Eq. (A1), we easily get that $\phi_i\geqslant 1$. Combined with Eq. (A8), the following closed-loop system can be obtained as:

$$\begin{aligned}\dot{s}_1 =&\phi_1[\gamma_1(g_1(\bar{\boldsymbol{x}}_1)x_2+f_1(\bar{\boldsymbol{x}}_1)+d_1-\dot{y}_0)-k_1\dot{\rho}_1]+\lambda_1\mathrm{sign}(\omega_1)\\ =&\phi_1[g_1(\bar{\boldsymbol{x}}_1)x_2-(1-\gamma_1)g_1(\bar{\boldsymbol{x}}_1)x_2+\gamma_1(f_1(\bar{\boldsymbol{x}}_1)+d_1-\dot{y}_0)-k_1\dot{\rho}_1]+\lambda_1\mathrm{sign}(\omega_1)\\ =&\phi_1[g_1(\bar{\boldsymbol{x}}_1)\beta_1-g_1(\bar{\boldsymbol{x}}_1)z_1-(1-\gamma_1)g_1(\bar{\boldsymbol{x}}_1)x_2+\Omega_1'],\end{aligned}\tag{A19}$$

where

$$\Omega_1' =g_1(\bar{\boldsymbol{x}}_1)e_2+\gamma_1(f_1(\bar{\boldsymbol{x}}_1)+d_1-\dot{y}_0)-k_1\dot{\rho}_1+\frac{\lambda_1\mathrm{sign}(\omega_1)}{\phi_1}.\tag{A20}$$

Similarly, we have

$$\begin{aligned}\dot{s}_i =&\phi_i[\gamma_i\left(g_i(\bar{\boldsymbol{x}}_i)x_{i+1}+f_i(\bar{\boldsymbol{x}}_i)-f_i(\bar{\boldsymbol{y}}_i)+f_i(\bar{\boldsymbol{y}}_i)+d_i-\frac{z_{i-1}}{\bar{d}_{i-1}}\right)-k_i\dot{\rho}_i]+\lambda_i\mathrm{sign}(\omega_i)\\ =&\phi_i[g_i(\bar{\boldsymbol{x}}_i)x_{i+1}-(1-\gamma_i)g_i(\bar{\boldsymbol{x}}_i)x_{i+1}+\gamma_i\left(f_i(\bar{\boldsymbol{x}}_i)-f_i(\bar{\boldsymbol{y}}_i)+f_i(\bar{\boldsymbol{y}}_i)+d_i-\frac{z_{i-1}}{\bar{d}_{i-1}}\right)-k_i\dot{\rho}_i]+\lambda_i\mathrm{sign}(\omega_i)\\ =&\phi_i[g_i(\bar{\boldsymbol{x}}_i)\beta_i-g_i(\bar{\boldsymbol{x}}_i)z_i-(1-\gamma_i)g_i(\bar{\boldsymbol{x}}_i)x_{i+1}+\gamma_i(f_i(\bar{\boldsymbol{x}}_i)-f_i(\bar{\boldsymbol{y}}_i))-\gamma_i\frac{z_{i-1}}{d_{i-1}}+\Omega_i'],\ i=2,3,\dots,n-1,\end{aligned}\tag{A21}$$

$$\begin{aligned}\dot{s}_n =&\phi_n[\gamma_n\left(g_n(\bar{\boldsymbol{x}}_n)\tau(t)v+g_n(\bar{\boldsymbol{x}}_n)\theta(t)+f_n(\bar{\boldsymbol{x}}_n)-f_n(\bar{\boldsymbol{y}}_n)+f_n(\bar{\boldsymbol{y}}_n)+d_n(t)-\frac{z_{n-1}}{\bar{d}_{n-1}}\right)-k_n\dot{\rho}_n]+\lambda_n\mathrm{sign}(\omega_n)\\ =&\phi_n[\gamma_n\left(g_n(\bar{\boldsymbol{x}}_n)\tau(t)v+f_n(\bar{\boldsymbol{x}}_n)-f_n(\bar{\boldsymbol{y}}_n)-\frac{z_{n-1}}{\bar{d}_{n-1}}\right)+\Omega_n'],\end{aligned}\tag{A22}$$

where

$$\Omega_i' =g_i(\bar{\boldsymbol{x}}_i)e_{i+1}+\gamma_i(f_i(\bar{\boldsymbol{y}}_i)+d_i)-k_i\dot{\rho}_i+\frac{\lambda_i\mathrm{sign}(\omega_i)}{\phi_i},\ i=2,3,\dots,n-1,\tag{A23}$$

$$\Omega_n' =\gamma_n(g_n(\bar{\boldsymbol{x}}_n)\theta(t)+f_n(\bar{\boldsymbol{y}}_n)+d_n)-k_n\dot{\rho}_n+\frac{\lambda_n\mathrm{sign}(\omega_n)}{\phi_n}.\tag{A24}$$

Then, we prove the boundedness of $\Omega_i'$. For $t\in[0,t_{\max})$, $k_i\in\Xi$ implies $\frac{\arctan(e_i)}{\rho_i}\in\Xi$. When $t\in[\frac{t_{\max}}{2},t_{\max})$, the definition of $\rho_i$ yields the bound $|e_i|\leqslant\tan(\rho_i(\frac{t_{\max}}{2}))$. Since $e_i$ is continuous in $t$, it is bounded on $[0,\frac{t_{\max}}{2}]$. Consequently, $e_i$ remains bounded on $[0,t_{\max})$. The continuity of $f_i(\cdot)$ and Assumption 1 ensure $f_i(\bar{\boldsymbol{y}}_n)$ is bounded on $[0,t_{\max})$. From Assumptions 1-4 and the boundedness of $e_2$, $\dot{\rho}_1$, it follows that $\Omega_1'$ is bounded on $[0,t_{\max})$. Similarly, $\Omega_2',\dots,\Omega_n'$ are bounded on $[0,t_{\max})$. Then, define $\Omega_i$, $(i=1,2,\dots,n)$ as:

$$\Omega_1=\Omega_1'+\mathrm{sign}(\xi_1)\frac{\bar{g}_1^2}{2},\tag{A25}$$

$$\Omega_i=\frac{1}{\underline{g}_i}\Omega_i'+\frac{\bar{g}_i^2\varrho_i'|\xi_i|\phi_i+1}{2\xi_i\underline{g}_i^2\varrho_i'\phi_i},\ i=2,3,\dots,n-1,\tag{A26}$$

$$\Omega_n=\frac{1}{\tau_f\underline{g}_n}\Omega_n'+\frac{1}{2\xi_n\tau_f^2\underline{g}_n^2\varrho_n'\phi_n};\tag{A27}$$

From the definition of $\xi_i$, we get the boundedness of $\xi_i$ for $i=2,3,\dots,n$. From the boundedness of $\bar{g}_i$, $\underline{g}_i$, $(i=1,2,\dots,n)$, $\varrho_i'$, $\varrho_i''$, $\tau_f$, $\Omega_i'$, $\xi_i$, $(i=2,3,\dots,n)$, we obtain $\Omega_i$ is bounded for $i=1,2,\dots,n$. Therefore, $|\Omega_i|\leqslant\bar{\Omega}_i$, $(i=1,2,\dots,n)$ for some unknown positive constants $\bar{\Omega}_i>0$ on $[0,t_{\max})$.

Then, consider the following Lyapunov function:

$$V = \sum_{i=1}^{n} V_i,$$

where $V_1 = \frac{1}{2}s_1^2$, $V_n = \frac{1}{\tau_f \underline{g}_n}(s_n + \varrho_n|s_n|)$, $V_i = \frac{1}{\underline{g}_i}(s_i + \varrho_i|s_i|)$, $(i = 2, 3, \ldots, n-1)$. Differentiating $V_1$ along with Eqs. (A19) and (A20), we obtain

$$\dot{V}_1 = \xi_1\phi_1(g_1(\bar{\boldsymbol{x}}_1)\beta_1 - g_1(\bar{\boldsymbol{x}}_1)z_1 - (1-\gamma_1)g_1(\bar{\boldsymbol{x}}_1)x_2 + \Omega_1').$$

Then, combining Eq. (A10) and the boundedness and definition of $\Omega_i$ in Eq. (A25), we get

$$\begin{aligned}
\dot{V}_1 \leqslant& -\sqrt{2}c_1\phi_1 g_1(\bar{\boldsymbol{x}}_1)\sqrt{V_1} + |\xi_1|\phi_1 z_1^2 + |\xi_1|\phi_1 x_2^2 + \frac{|\xi_1|\phi_1\bar{g}_1^2}{2} + \xi_1\phi_1\Omega_1' \\
=& -\sqrt{2}c_1\phi_1 g_1(\bar{\boldsymbol{x}}_1)\sqrt{V_1} + |\xi_1|\phi_1(z_1^2 + x_2^2) + \xi_1\phi_1\left(\Omega_1' + \mathrm{sign}(\xi_1)\frac{\bar{g}_1^2}{2}\right) \\
\leqslant& -\sqrt{2}c_1\phi_1\underline{g}_1\sqrt{V_1} + |\xi_1|\phi_1(z_1^2 + x_2^2) + |\xi_1|\phi_1\bar{\Omega}_1.
\end{aligned} \tag{A28}$$

Similarly, taking the right Dini upper derivatives of $V_i$, $(i = 2, 3, \ldots, n-1)$ along with Eqs. (A21) and (A23), then substituting $\beta_i$ with using Eq. (A11) and applying Eq. (A26), we have

$$\begin{aligned}
D^+V_i =& \frac{\xi_i}{\underline{g}_i}\phi_i[g_i(\bar{\boldsymbol{x}}_i)\beta_i - g_i(\bar{\boldsymbol{x}}_i)z_i - (1-\gamma_i)g_i(\bar{\boldsymbol{x}}_i)x_{i+1} + \gamma_i(f_i(\bar{\boldsymbol{x}}_i) - f_i(\bar{\boldsymbol{y}}_i)) - \gamma_i\frac{z_{i-1}}{d_{i-1}} + \Omega_i'] \\
\leqslant& \frac{g_i(\bar{\boldsymbol{x}}_i)}{\underline{g}_i}\xi_i\phi_i\beta_i + \frac{\bar{g}_i}{\underline{g}_i}|\xi_i|\phi_i|z_i| + \frac{\bar{g}_i}{\underline{g}_i}|\xi_i|\phi_i|x_{i+1}| + \frac{1}{2\underline{g}_i^2\varrho_i'} \\
&+ \varrho_i'\xi_i^2\phi_i^2(f_i(\bar{\boldsymbol{x}}_i) - f_i(\bar{\boldsymbol{y}}_i))^2 + \varrho_i'\xi_i^2\phi_i^2\frac{z_{i-1}^2}{d_{i-1}^2} + \frac{1}{\underline{g}_i}\xi_i\phi_i\Omega_i' \\
\leqslant& \frac{g_i(\bar{\boldsymbol{x}}_i)}{\underline{g}_i}\xi_i\phi_i\beta_i + \frac{\bar{g}_i^2\varrho_i'|\xi_i|\phi_i + 1}{2\underline{g}_i^2\varrho_i'} + |\xi_i|\phi_i(z_i^2 + x_{i+1}^2) \\
&+ \varrho_i'\xi_i^2\phi_i^2\left((f_i(\bar{\boldsymbol{x}}_i) - f_i(\bar{\boldsymbol{y}}_i))^2 + \frac{z_{i-1}^2}{d_{i-1}^2}\right) + \frac{1}{\underline{g}_i}\xi_i\phi_i\Omega_i' \\
=& \frac{g_i(\bar{\boldsymbol{x}}_i)}{\underline{g}_i}\xi_i\phi_i\beta_i + |\xi_i|\phi_i(z_i^2 + x_{i+1}^2) \\
&+ \varrho_i'\xi_i^2\phi_i^2(\left(f_i(\bar{\boldsymbol{x}}_i) - f_i(\bar{\boldsymbol{y}}_i))^2 + \frac{z_{i-1}^2}{d_{i-1}^2}\right) + \xi_i\phi_i\left(\frac{1}{\underline{g}_i}\Omega_i' + \frac{\bar{g}_i^2\varrho_i'|\xi_i|\phi_i + 1}{2\xi_i\underline{g}_i^2\varrho_i'\phi_i}\right) \\
\leqslant& -c_i\phi_i\sqrt{\underline{g}_i}\sqrt{V_i} - |\xi_{i-1}|\phi_{i-1}(z_{i-1}^2 + x_i^2) + |\xi_i|\phi_i(z_i^2 + x_{i+1}^2) + |\xi_i|\phi_i\bar{\Omega}_i.
\end{aligned} \tag{A29}$$

For $V_n$, combining Eqs. (A22), (A24), (A12) and (A27) and its right Dini upper derivative, we obtain

$$\begin{aligned}
D^+V_n \leqslant& \frac{1}{\tau_f\underline{g}_n}\xi_n\phi_n\gamma_n g_n(\bar{\boldsymbol{x}}_n)\tau(t)v + \frac{1}{2\tau_f^2\underline{g}_n^2\varrho_n'} + \varrho_n'\xi_n^2\phi_n^2(f_n(\bar{\boldsymbol{x}}_n) - f_n(\bar{\boldsymbol{y}}_n))^2 \\
&+ \varrho_n'\xi_n^2\phi_n^2\frac{z_{n-1}^2}{d_{n-1}^2} + \frac{1}{\tau_f\underline{g}_n}\xi_n\phi_n\Omega_n' \\
=& \frac{1}{\tau_f\underline{g}_n}\xi_n\phi_n\gamma_n g_n(\bar{\boldsymbol{x}}_n)\tau(t)v' + \varrho_n'\xi_n^2\phi_n^2(f_n(\bar{\boldsymbol{x}}_n) - f_n(\bar{\boldsymbol{y}}_n))^2 \\
&+ \varrho_n'\xi_n^2\phi_n^2\frac{z_{n-1}^2}{d_{n-1}^2} + \xi_n\phi_n\left(\frac{1}{\tau_f\underline{g}_n}\Omega_n' + \frac{1}{2\xi_n\tau_f^2\underline{g}_n^2\varrho_n'\phi_n}\right) \\
\leqslant& -c_n\phi_n\sqrt{\tau_f\underline{g}_n}\sqrt{V_n} - |\xi_{n-1}|\phi_{n-1}(z_{n-1}^2 + x_n^2) - \sum_{i=1}^{n}|\xi_i|\phi_i H_i + |\xi_n|\phi_n\bar{\Omega}_n.
\end{aligned} \tag{A30}$$

Therefore, combining Eqs. (A28)-(A30), we get

$$\begin{aligned}
D^+V \leqslant& -\sqrt{2}c_1\phi_1\underline{g}_1\sqrt{V_1} - \sum_{i=2}^{n-1}c_i\phi_i\sqrt{\underline{g}_i}\sqrt{V_i} - c_n\phi_n\sqrt{\tau_f\underline{g}_n}\sqrt{V_n} + \sum_{i=1}^{n}|\xi_i|\phi_i(\bar{\Omega}_i - H_i) \\
\leqslant& -aV^{\frac{1}{2}} + \sum_{i=1}^{n}|\xi_i|\phi_i(\bar{\Omega}_i - H_i),
\end{aligned} \tag{A31}$$

where $a = \min\{\sqrt{2}c_1\phi_1\underline{g}_1, c_2\phi_2\sqrt{\underline{g}_2}, \cdots, c_n\phi_n\sqrt{\tau_f\underline{g}_n}\}$.

## Appendix A.2 The proof of Theorem 1

*Proof.* To begin with the proof of Theorem 1, we prove the $\forall t \in [0,+\infty)$, $|e_i(t)| < \tan(\rho_i(t))$, $(i = 1,2,\dots,n)$. According to Eqs. (A6) and (A7), we only need to prove that there exists $\bar{\omega}_i > 0$ such that $|\omega_i| \leqslant \bar{\omega}_i$, for $t \in [0,+\infty)$. Then we can easily obtain

$$-1 < -\bar{k}_i \leqslant k_i \leqslant \bar{k}_i < 1, \tag{A32}$$

where $\bar{k}_i \triangleq \frac{2}{\pi}\arctan(\bar{\omega}_i)$. By seeking a contradiction, suppose that there exists $\omega_j$, $j \in \{1,2,\dots,n\}$ unbounded on $[0,t_{\max})$. Then we have $\lim_{t\to t_2} \|\omega\|_t = +\infty$, $t_2 \in (0,t_{\max}]$. Thus, there exist $0 \leqslant t_1 < t_2$ such that

$$\|\omega\|_{t_1} \geqslant \frac{\bar{\Omega}_i}{r_i e^{-\bar{r}_i t_1}}. \tag{A33}$$

Therefore, when $t \in [t_1,t_2)$,

$$H_i(t) \geqslant r_i \frac{\bar{\Omega}_i}{r_i e^{-\bar{r}_i t_1}} e^{-\bar{r}_i t_1} = \bar{\Omega}_i. \tag{A34}$$

Combining Eq. (A34) with Eq. (A31), we have

$$D^+V \leqslant -aV^{\frac{1}{2}},\ \forall t \in [t_1,t_2), \tag{A35}$$

which means $s_i$, $(i = 1,2,\dots,n)$ are bounded on $[t_1,t_2)$. Furthermore, according to the boundedness of $\|\omega\|_t$, $t \in [0,t_1]$ and Eq. (A8), we can obtain that $s_i$, $(i = 1,2,\dots,n)$ are bounded on $[0,t_2)$. From Lemma 1 in [11], we have $\omega_i$, $(i = 1,2,\dots,n)$ are bounded on $[0,t_2)$, which contradicts $\lim_{t\to t_2} \|\omega\|_t = +\infty$. Therefore, for all $t \in [0,t_{\max})$, Eq. (A32) holds, which implies $k_i \in [-\bar{k}_1,\bar{k}_1] \times \cdots \times [-\bar{k}_n,\bar{k}_n] \subset \Xi$. We can conclude that $t_{\max} = +\infty$ by Proposition C.3.6 of [12]. Then, we have $\forall t \in [0,+\infty)$, $|e_i(t)| < \tan(\rho_i(t))$, $(i = 1,2,\dots,n)$.

Next, we turn to the sliding motion occurs within a finite time. Suppose that there does not exist a $T$ such that $s_i \equiv 0$, $\forall t \in [T,+\infty)$. There are three cases satisfying this assumption.

*Case A*: If there is no switching for all $t \in [0,+\infty)$, as shown in Eq. (A14), $h_i(t)$ keeps increasing and $\dot{h}_i(t) \geqslant h_{i2}$. Then, there exists an instant $t_3 \geqslant \frac{\bar{\Omega}_i}{h_{i2}}$ such that $H_i(t) \geqslant h_i(t) \geqslant \bar{\Omega}_i, \forall t \in [t_3,+\infty)$. Therefore, Eq. (A35) holds for $t \in [t_3,+\infty)$, which leads to $s_i$ converging to zero within a finite time $\bar{T} \leqslant t_3 + \frac{2V^{\frac{1}{2}}(t_3)}{a}$, thus resulting in a contradiction.

*Case B*: If there exists a finite switching series $\{t_q\}_{q=1}^{p}$, where $p$ is finite, then $h_i(t)$ stops switching. Combining the expression of $s(t)$, we get $s(t) > 0$ for all $t \in (t_p,+\infty)$, which implies that $h_i(t)$ evolves according to Eq. (A14) after $t_p$. Similar to the proof in *Case A*, this is also a contradiction.

*Case C*: If there exists an infinite switching series $\{t_q\}_{q=1}^{\infty}$, then $h_i(t)$ keeps switching during $t \in [0,+\infty)$. Then, there exist $0 \leqslant \bar{t}_1 < \infty$ such that

$$|Q_{\bar{t}_1}| \geqslant \frac{\bar{\Omega}_i}{r_i e^{-\bar{r}_i \bar{t}_1}}. \tag{A36}$$

Therefore, when $t \in [\bar{t}_1,+\infty)$,

$$H_i(t) \geqslant r_i \frac{\bar{\Omega}_i}{r_i e^{-\bar{r}_i \bar{t}_1}} e^{-\bar{r}_i \bar{t}_1} = \bar{\Omega}_i. \tag{A37}$$

This also implies that Eq. (A35) holds for $t \in [\bar{t}_1,+\infty)$. Similar to the proof in *Case A*, this is a contradiction. To sum up, the sliding mode occurs within a finite time. When the sliding mode occurs within a finite time, we have that there exists a $T$ such that $s_i \equiv 0$, $\forall t \geqslant T$. Then, for $\forall t \geqslant T$, according to Eq. (A8), we get

$$\dot{\omega}_i + \lambda_i \mathrm{sign}(\omega_i) = 0. \tag{A38}$$

Then, we construct a Lyapunov function:

$$\bar{V} = \frac{1}{2}\omega_i^2.$$

Differentiating $\bar{V}$ and combining with Eq. (A38), we obtain that

$$\dot{\bar{V}} = -\lambda_i|\omega_i| \leqslant -\lambda_i\sqrt{2\bar{V}}. \tag{A39}$$

As a result, for $\forall t \geqslant T^* \triangleq T + \frac{1}{\lambda_i}\sqrt{2\bar{V}(T)}$, $\bar{V}(t) \equiv 0$, which means $\omega_i \equiv 0$, $\forall t > T^*$. Then, we obtain $e_i = 0$, $\forall t > T^*$ from Eqs. (A6) and (A7), which means the tracking error converges to zero within a finite time $T^*$.

Lastly, we prove the closed-loop signals are all globally bounded. The closed-loop signals include $x_i$, $s_i$, $\omega_i$, $k_i$, $z_i$, $\alpha_i$, $\beta_i$, $v$. From the proof above, we get the global boundedness of $k_i$, $\omega_i$, $s_i$, $e_i$, $x_1$. From Eqs. (A4) and (A10), $\beta_1$, $\alpha_1$ are bounded. Then, we get $x_2$, $z_1$ is bounded from Eqs. (A3) and (A5). Similarly, we obtain the boundedness of $x_i$, $(i = 3,4,\dots,n)$ and

$\alpha_i$, $\beta_i$, $z_i$, $(i = 2, 3, \ldots, n)$. The boundedness of the controller $v$ depends on $H_i$. Firstly, when $t \in [0, T^*)$, $h_i$ is bounded since $T^*$ is bounded. Then, when $t \in [T^*, +\infty)$, $h_i$ is bounded according to Eq. (A15). Since $r_i(\|\omega\|_t + |Q_t|)e^{-\bar{r}_i t}$ is bounded for $\forall t \in [0, +\infty)$, we have $H_i$ is bounded which means $v$ is bounded. In conclusion, the closed-loop signals are all globally bounded. To summarize, all three control objectives are satisfied: First, the output $y(t)$ tracks the reference signal $y_0(t)$ with prescribed performance; Second, exact tracking is guaranteed within a finite time; Third, all signals in the closed-loop system are uniformly bounded globally. ■

**Remark 2.** Theorem 1's proof shows that the feedback gain $H_i$ is introduced to handle the uncertainty $\Omega_i$ with unknown upper bound. Here, $h_i$ is designed to drive the sliding variable $s_i$ to the sliding surface $s_i = 0$ and maintain it there within a finite time. The term $r_i\|\omega\|_t e^{-\bar{r}_i t}$ is incorporated to prevent finite-time escape of $s_i$ from the sliding surface, while the latter term $r_i|Q_t|e^{-\bar{r}_i t}$ in Eq. (A13) suppresses infinite switching. Multiple tunable parameters exist in the prescribed performance function and the control scheme. Based on linear filter theory in sliding mode control, the filter parameters $\bar{d}_i$ and $\bar{\tau}_i$ should be chosen sufficiently small to achieve satisfactory approximation accuracy. The performance function parameters $\rho_{i1}$ and $\rho_{i\infty}$ should be selected according to practical requirements, under the constraint $0 < \rho_{i\infty} < \frac{\pi}{2}$. Generally, a larger value of $\rho_{i1}$ yields faster convergence, while a smaller $\rho_{i\infty}$ leads to improved tracking performance. As indicated by Eq. (A31) and the proof of Theorem 1, the parameters $c_i$, $r_i$, $\bar{r}_i$, $\bar{h}_{i1}$, and $\bar{h}_{i2}$ have a significant influence on the settling time of the sliding motion. Specifically, a smaller $\bar{r}_i$ together with larger values of $c_i$, $r_i$, $\bar{h}_{i1}$, and $\bar{h}_{i2}$ results in a reduced settling time.

**Remark 3.** In this remark, we demonstrate that the proposed control method is also applicable to cases with sensor faults. We consider the following model defined in [13] in detail:

$$y(t) = K(t)x_1(t) + B(t),$$

where $0 < \bar{K} \leqslant K(t) \leqslant 1$ represents the loss of effectiveness, and $B(t)$ depicts bias, drift and loss of accuracy. Both $\dot{K}(t)$, $B(t)$ and $\dot{B}(t)$ are bounded. Then we let $e_1(t) = y(t) - y_0(t) = K(t)x_1(t) + B(t) - y_0(t)$. Taking the derivative of $e_1$, and combining it with Eq. (A2), we have $\dot{e}_1 = \frac{1}{\cos^2(k_1\rho_1)}(\dot{k}_1\rho_1 + k_1\dot{\rho}_1) = K(g_1(\bar{\boldsymbol{x}}_1)x_2 + f_1(\bar{\boldsymbol{x}}_1) + d_1) + \dot{K}x_1 + \dot{B} - \dot{y}_0$. Then, we get

$$\begin{aligned}\dot{k}_1 =& \frac{1}{\rho_1}[\gamma_1\left(K(g_1(\bar{\boldsymbol{x}}_1)x_2 + f_1(\bar{\boldsymbol{x}}_1) + d_1) + \dot{K}x_1 + \dot{B} - \dot{y}_0\right) - k_1\dot{\rho}_1]\\ =& \frac{1}{\rho_1}[\gamma_1 K g_1(\bar{\boldsymbol{x}}_1)(\tan(k_2\rho_2) + \beta_1 - z_1) + \gamma_1\left(K(f_1(\bar{\boldsymbol{x}}_1) + d_1) + \dot{B} - \dot{y}_0\right) - k_1\dot{\rho}_1].\end{aligned} \tag{A40}$$

Similarly, from Eq. (A6), we have $\dot{\omega}_i = \frac{\pi}{2\cos^2(\frac{\pi}{2}k_i)}\dot{k}_i$. Let $\phi_i = \frac{\pi}{2\rho_i\cos^2(\frac{\pi}{2}k_i)}$, $(i = 1, 2, \ldots, n)$. Combined with Eqs. (A8) and (A40), the following closed-loop system can be obtained as:

$$\begin{aligned}\dot{s}_1 =& \phi_1[\gamma_1\left(K(g_1(\bar{\boldsymbol{x}}_1)x_2 + f_1(\bar{\boldsymbol{x}}_1) + d_1) + \dot{K}x_1 + \dot{B} - \dot{y}_0\right) - k_1\dot{\rho}_1] + \lambda_1\mathrm{sign}(\omega_1)\\ =& \phi_1[g_1(\bar{\boldsymbol{x}}_1)x_2 - (1 - \gamma_1 K)g_1(\bar{\boldsymbol{x}}_1)x_2 + \gamma_1\left(K(f_1(\bar{\boldsymbol{x}}_1) + d_1) + \dot{K}x_1 + \dot{B} - \dot{y}_0\right)\\ & - k_1\dot{\rho}_1] + \lambda_1\mathrm{sign}(\omega_1)\\ =& \phi_1[g_1(\bar{\boldsymbol{x}}_1)\beta_1 - g_1(\bar{\boldsymbol{x}}_1)z_1 - (1 - \gamma_1 K)g_1(\bar{\boldsymbol{x}}_1)x_2 + \Omega_1''],\end{aligned} \tag{A41}$$

where

$$\Omega_1'' = g_1(\bar{\boldsymbol{x}}_1)e_2 + \gamma_1\left(K(f_1(\bar{\boldsymbol{x}}_1) + d_1) + \dot{K}x_1 + \dot{B} - \dot{y}_0\right) - k_1\dot{\rho}_1 + \frac{\lambda_1\mathrm{sign}(\omega_1)}{\phi_1}. \tag{A42}$$

Following the same reasoning as in the proof of the boundedness of $\Omega_i'$, it can be concluded that $\Omega_1''$ is bounded. Define $\Omega_1''' = \Omega_1'' + \mathrm{sign}(\xi_1)\frac{\bar{g}_1^2}{2}$, and since both terms on the right-hand side are bounded, $\Omega_1'''$ is also bounded. Therefore, there exists an unknown positive constant $\bar{\Omega}_1' > 0$ such that $|\Omega_1'''| \leqslant \bar{\Omega}_1'$ holds on the interval $[0, t_{\max})$.

Consider the same Lyapunov function: $V = \sum_{i=1}^n V_i$, where $V_1 = \frac{1}{2}s_1^2$, $V_n = \frac{1}{\tau_f \underline{g}_n}(s_n + \varrho_n|s_n|)$, $V_i = \frac{1}{\underline{g}_i}(s_i + \varrho_i|s_i|)$, $(i = 2, 3, \ldots, n-1)$. Differentiating $V_1$ along with Eqs. (A41) and (A42), we obtain

$$\dot{V}_1 = \xi_1\phi_1(g_1(\bar{\boldsymbol{x}}_1)\beta_1 - g_1(\bar{\boldsymbol{x}}_1)z_1 - (1 - \gamma_1 K)g_1(\bar{\boldsymbol{x}}_1)x_2 + \Omega_1'').$$

Then, combining Eq. (A10) and the boundedness and the definition of $\Omega_i'''$, we get

$$\begin{aligned}\dot{V}_1 \leqslant& -\sqrt{2}c_1\phi_1 g_1(\bar{\boldsymbol{x}}_1)\sqrt{V_1} + |\xi_1|\phi_1 z_1^2 + |\xi_1|\phi_1 x_2^2 + \frac{|\xi_1|\phi_1\left(1 + (1 - \gamma_1 K)^2\right)\bar{g}_1^2}{4} + \xi_1\phi_1\Omega_1'\\ \leqslant& -\sqrt{2}c_1\phi_1 g_1(\bar{\boldsymbol{x}}_1)\sqrt{V_1} + |\xi_1|\phi_1(z_1^2 + x_2^2) + \xi_1\phi_1\left(\Omega_1'' + \mathrm{sign}(\xi_1)\frac{\bar{g}_1^2}{2}\right)\\ \leqslant& -\sqrt{2}c_1\phi_1\underline{g}_1\sqrt{V_1} + |\xi_1|\phi_1(z_1^2 + x_2^2) + |\xi_1|\phi_1\bar{\Omega}_1'.\end{aligned} \tag{A43}$$

The second inequality follows from the fact that $(1 - \gamma_1 K)^2 \leqslant 1$ for $K$ and $\gamma_1$ both lying in the interval $(0, 1]$. $V_i$, $\Omega_i$, $s_i$, $k_i$, $(i = 2, 3, \ldots, n)$ are the same with those above. With Eq. (A43), we can conclude that the controller and adaptive laws designed in Eqs. (A10)-(A12) are also applicable to the system containing sensor faults.

## Appendix A.3 Control design and the proof of Theorem 2

In this subsection, we consider the case where the directions of virtual control signals $g_i$, $(i = 1, 2, \ldots, n-1)$ are unknown while Assumption 6 holds. The virtual signals $\beta_i$ and actual controller $v$ of unknown virtual control directions:

$$\beta_1 = -c_1 \frac{\text{sign}(\xi_1)}{b_1}, \tag{A44}$$

$$\beta_i = -\frac{c_i\sqrt{s_i + \varrho_i|s_i|}}{b_i\xi_i} - \frac{\text{sign}(\xi_i)}{b_i}\left(\bar{L}_i + \frac{|z_{i-1}|}{\bar{d}_{i-1}}\right) - \frac{|\xi_{i-1}|\phi_{i-1}(z_{i-1}^2 + x_i^2)}{b_i\xi_i\phi_i},\ i = 2, 3, \ldots, n-1, \tag{A45}$$

$$v = -\frac{1}{\gamma_n}\left(\frac{c_n\sqrt{s_n + \varrho_n|s_n|}}{\xi_n} + \varrho_n'\left(\bar{L}_n^2 + \frac{z_{n-1}^2}{\bar{d}_{n-1}^2}\right) + \frac{|\xi_{n-1}|\phi_{n-1}(z_{n-1}^2 + x_n^2)}{\xi_n\phi_n} + \sum_{i=1}^{n}\frac{|\xi_i|\phi_i H_i}{\xi_n\phi_n}\right), \tag{A46}$$

where $c_i > 0$, $(i = 1, 2, \ldots, n)$, $\varrho_i > 1$, $(i = 2, 3, \ldots, n)$, $\varrho_n' > 0$ are scalars to be designed. Variables $\xi_i$, $\phi_i$, $\bar{L}_i$ and feedback $H_i$ are the same in Appendix A.1. Similarly, the following closed-loop systems can thus be obtained:

$$\begin{aligned}\dot{s}_1 =& \phi_1[b_1x_2 + (\gamma_1g_1(\bar{\boldsymbol{x}}_1) - b_1)x_2 + \gamma_1(f_1(\bar{\boldsymbol{x}}_1) + d_1 - \dot{y}_0) - k_1\dot{\rho}_1(t)] + \lambda_1\text{sign}(\omega_1)\\ =& \phi_1[b_1\beta_1 - b_1z_1 + (\gamma_1g_1(\bar{\boldsymbol{x}}_1) - b_1)x_2 + \Omega_1'],\end{aligned} \tag{A47}$$

$$\dot{s}_i = \phi_i[b_i\beta_i - b_iz_i + (\gamma_ig_i(\bar{\boldsymbol{x}}_i) - b_i)x_{i+1} + \gamma_i(f_i(\bar{\boldsymbol{x}}_i) - f_i(\bar{\boldsymbol{y}}_i)) - \gamma_i\frac{z_{i-1}}{d_{i-1}} + \Omega_i'],\ i = 2, 3, \ldots, n-1, \tag{A48}$$

$$\dot{s}_n = \phi_n[\gamma_n\left(g_n(\bar{\boldsymbol{x}}_n)\tau(t)v + f_n(\bar{\boldsymbol{x}}_n) - f_n(\bar{\boldsymbol{y}}_n) - \frac{z_{n-1}}{\bar{d}_{n-1}}\right) + \Omega_n'], \tag{A49}$$

where $b_i$ are nonzero constants which can be designed arbitrarily, and $\Omega_i'$ is defined in Eqs. (A50), (A51) and (A52).

$$\Omega_1' = b_1e_2 + \gamma_1(f_1(\bar{\boldsymbol{x}}_1) + d_1 - \dot{y}_0) - k_1\dot{\rho}_1 + \frac{\lambda_1\text{sign}(\omega_1)}{\phi_1}, \tag{A50}$$

$$\Omega_i' = b_ie_{i+1} + \gamma_i(f_i(\bar{\boldsymbol{y}}_i) + d_i) - k_i\dot{\rho}_i + \frac{\lambda_i\text{sign}(\omega_i)}{\phi_i},\ i = 2, 3, \ldots, n-1, \tag{A51}$$

$$\Omega_n' = \gamma_n(g_n(\bar{\boldsymbol{x}}_n)\theta(t) + f_n(\bar{\boldsymbol{y}}_n) + d_n) - k_n\dot{\rho}_n + \frac{\lambda_n\text{sign}(\omega_n)}{\phi_n}. \tag{A52}$$

The proof of the boundedness of $\Omega_i'$ is similar to that in Appendix A.1. Define $\Omega_i^*$ as:

$$\Omega_i^* = \Omega_i' + \text{sign}(\xi_i)\frac{3b_i^2 + 2\bar{g}_i^2}{4},\ i = 1, 2, \ldots, n-1, \tag{A53}$$

$$\Omega_n^* = \frac{\xi_n\phi_n}{\tau_f\underline{g}_n}\Omega_n' + \frac{1}{2\tau_f^2\underline{g}_n^2\varrho_n'}. \tag{A54}$$

Then, we can easily have $\Omega_i^*$ are bounded, for $i = 1, 2, \ldots, n$. Therefore, $|\Omega_i^*| \leqslant \bar{\Omega}_i^*$, $(i = 1, 2, \ldots, n)$ for some unknown positive constants $\bar{\Omega}_i^* > 0$ on $[0, t_{\max})$. Consider the following Lyapunov function:

$$V = \sum_{i=1}^{n} V_i,$$

where $V_1 = \frac{1}{2}s_1^2$, $V_n = \frac{1}{\tau_f\underline{g}_n}(s_n + \varrho_n|s_n|)$, $V_i = s_i + \varrho_i|s_i|$, $(i = 2, 3, \ldots, n-1)$. Differentiating $V_1$ with using Eqs. (A47), (A44) and (A53), we obtain

$$\begin{aligned}\dot{V}_1 =& \xi_1\phi_1(b_1\beta_1 - b_1z_1 - (\gamma_1g_1(\bar{\boldsymbol{x}}_1) - b_1)x_2 + \Omega_1')\\ \leqslant& -\sqrt{2}c_1\phi_1\sqrt{V_1} + |\xi_1|\phi_1z_1^2 + |\xi_1|\phi_1x_2^2 + |\xi_1|\phi_1\frac{3b_1^2}{4} + |\xi_1|\phi_1\frac{\bar{g}_1^2}{2} + \xi_1\phi_1\Omega_1'\\ \leqslant& -\sqrt{2}c_1\phi_1\sqrt{V_1} + |\xi_1|\phi_1(z_1^2 + x_2^2) + |\xi_1|\phi_1\bar{\Omega}_1^*.\end{aligned} \tag{A55}$$

Similarly, taking the right Dini upper derivatives of $V_i$, $(i = 2, 3, \ldots, n-1)$ along with Eq. (A48) and substituting $\beta_i$ with using Eq. (A45) and applying Eq. (A53), we have

$$\begin{aligned}D^+V_i \leqslant& \xi_i\phi_ib_i\beta_i + |\xi_i|\phi_i(z_i^2 + x_{i+1}^2) + \phi_i\frac{3b_i^2 + 2\bar{g}_i^2}{4} + |\xi_i|\phi_i\left(|f_i(\bar{\boldsymbol{x}}_i) - f_i(\bar{\boldsymbol{y}}_i)| + \frac{|z_{i-1}|}{\bar{d}_{i-1}}\right) + \xi_i\phi_i\Omega_i'\\ \leqslant& -c_i\phi_i\sqrt{V_i} - |\xi_{i-1}|\phi_{i-1}(z_{i-1}^2 + x_i^2) + |\xi_i|\phi_i(z_i^2 + x_{i+1}^2) + |\xi_i|\phi_i\bar{\Omega}_i^*.\end{aligned} \tag{A56}$$

For $V_n$, combining Eqs. (A49), (A46), (A54) and its right Dini upper derivative, we obtain

$$D^+V_n \leqslant -c_n\phi_n\sqrt{\tau_f\underline{g}_n}\sqrt{V_n} - |\xi_{n-1}|\phi_{n-1}(z_{n-1}^2 + x_n^2) - \sum_{i=1}^{n}|\xi_i|\phi_iH_i + |\xi_n|\phi_n\bar{\Omega}_n^*. \tag{A57}$$

Similarly, combining Eqs. (A55)-(A57), we have

$$\dot{V} \leqslant -a'V^{\frac{1}{2}} + \sum_{i=1}^{n} |\xi_i|\phi_i(\bar{\Omega}_i^* - H_i), \tag{A58}$$

where $a' = \min\{\sqrt{2}c_1\phi_1, c_2\phi_2, \cdots, c_n\sqrt{\tau_f \underline{g}_n}\phi_n\}$.

*Proof.* With Eqs. (A58), we can easily prove Theorem 2 following the proof of Theorem 1 in Appendix A.2. ■

**Remark 4.** Compared with methods that only ensure practical stability [3, 14, 15], asymptotic stability [4, 16, 17] or exponential stability [18], the proposed approach can achieve global performance-guaranteed finite-time exact-tracking control for uncertain strict-feedback nonlinear systems under simultaneous actuator faults and external disturbances. This is achieved through integral sliding mode techniques, which enable the establishment of prescribed transient and steady-state performance bounds. The feasibility and effectiveness of the proposed control scheme are demonstrated through various simulation examples and comparative studies provided in Appendix B.

## Appendix B Simulations

In this section, simulations and comparisons are presented to demonstrate the effectiveness of the proposed control methods of Theorem 1.

The first example is to verify the effectiveness of exact tracking within a finite time compared to the method in [3].

Consider the dynamics of that in [3]:

$$\begin{aligned} \dot{x}_1 &= x_2, \\ \dot{x}_2 &= f_2(\bar{x}_2, t) + g_2(\bar{x}_2)u, \end{aligned} \tag{B1}$$

with

$$f_2(\bar{x}_2, t) = \frac{g\sin(x_1) - \frac{mlx_2^2\sin(x_1)\cos(x_1)}{m+m_c}}{l(\frac{4}{3} - \frac{m\cos^2(x_1)}{m+m_c})}\eta(t),$$

$$g_2(\bar{x}_2) = \frac{\frac{1}{m+m_c}}{l(\frac{4}{3} - \frac{m\cos^2(x_1)}{m+m_c})},$$

where $x_1$, $x_2$, $l = 0.5$m, $m = 0.1$kg, $m_c = 1$kg are the angle of the pendulum, the angular velocity, the half length of a pole, the mass of a pole and a cart, respectively. $g = 9.8\text{m/s}^2$ is the gravitational acceleration. The existing component fault $\eta(t)$, and the actuator fault are the same with that in [3], which is

$$\eta(t) = \begin{cases} 1, & t < 15, \\ 4, & 15 \leqslant t \leqslant 20, \\ 2, & 20 \leqslant t \leqslant 25, \\ 5\sin(10t), & 25 \leqslant t \leqslant 30. \end{cases}$$

The actuator fault happens at $t = 10$s, i.e.,

$$u(t) = \begin{cases} v(t), & t < 10, \\ 0.5v(t) + 0.5, & t \geqslant 10. \end{cases}$$

The controller in [3] is denoted as $v'(t)$ for convenience. Let $\rho_1(t) = (\frac{\pi}{2} - 0.01)e^{-0.5t} + 0.01$ and $\rho_2(t) = (\frac{\pi}{2} - 0.5)e^{-0.5t} + 0.5$. For the purpose of rigor in simulations, the parameters of $v'(t)$ are set the same as that in [3]. The parameters in the bounding functions in [3] are set as 0.5. The reference signal is set as $y_0^1(t) = \sin(t)$. The parameters in $v(t)$ as shown in Eq. (A12) are set as $\bar{d}_1 = 0.01$, $\varrho_2 = 20$, $\varrho_2' = 0.01$, $\lambda_i = 1$, $\tau_i = 0.001$, $r_i = 1$, $\bar{r}_i = 10$, $\bar{h}_{ij} = 1$, $\bar{h}_{i3}(0) = 0$, where $i = 1, 2$, $j = 1, 2, 4$ and the initial value is chosen as $\bar{\boldsymbol{x}}_2^1(0) = [0.2, -0.2]^\top$. The simulation results are displayed in Figures. B1-B2.

Figure B1 presents the tracking errors $\arctan(e(t))$ and $\arctan(e^*(t))$ of system (B1) under the control laws $v(t)$ and $v'(t)$, respectively. Unlike the protocol $v'(t)$ from [3], which only guarantees uniformly bounded error (blue dashed line), our method $v(t)$ achieves finite-time convergence of the tracking error to zero while maintaining prescribed performance (red solid line).

Figure B2 compares the reference signal $y_0^1(t)$ with the output trajectories under the two control schemes. Here, the red solid line $y_1^1(t)$ and the blue dashed line $y_2^1(t)$ correspond to the outputs under $v(t)$ and $v'(t)$, respectively. It can be seen that the output under $v(t)$ tracks the reference signal more rapidly than under $v'(t)$, confirming both the effectiveness of the proposed method and its advantage over the existing approach.

**Remark 5.** It should be noted that system (B1) is intentionally designed without disturbances, since the comparative controller from [3] is only applicable to disturbance-free systems. The rest part verifies the proposed control signal's applicability to systems with external disturbances.

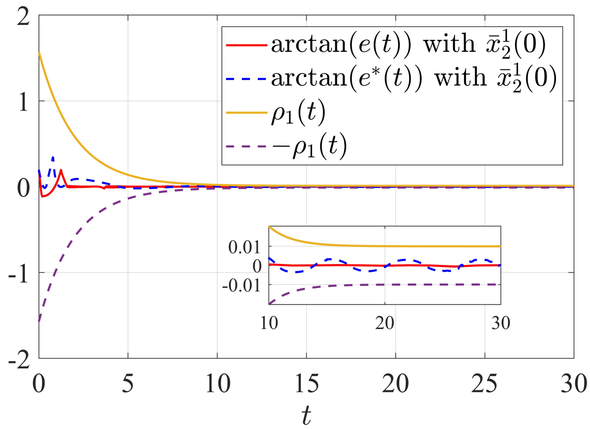


**Figure B1** Tracking errors $\arctan(e(t))$ and $\arctan(e^*(t))$ of system (B1) under the control of the proposed signal $v(t)$ in Eq. (A12) and $v'(t)$ in [3], respectively.

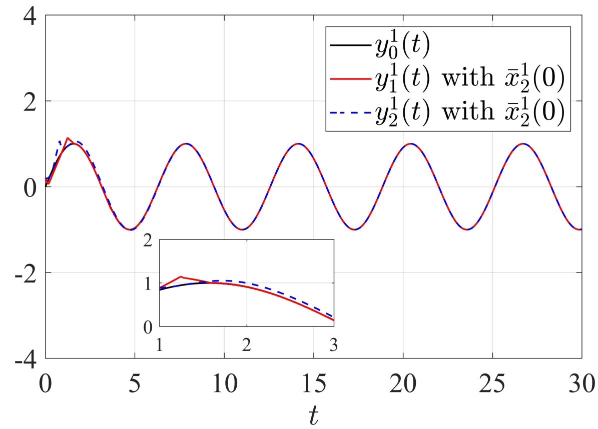


**Figure B2** Reference signal $y_0^1(t)$ and output trajectories.

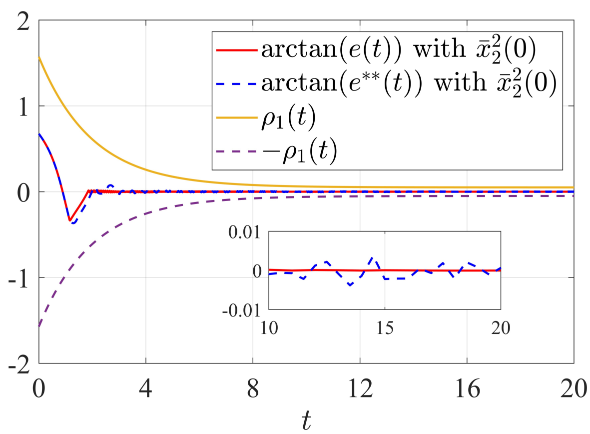


**Figure B3** Tracking errors $\arctan(e(t))$ and $\arctan(e^{**}(t))$ of system (B2) under the control of the proposed signal $v(t)$ in Eq. (A12) and $v''(t)$ in [11], respectively.

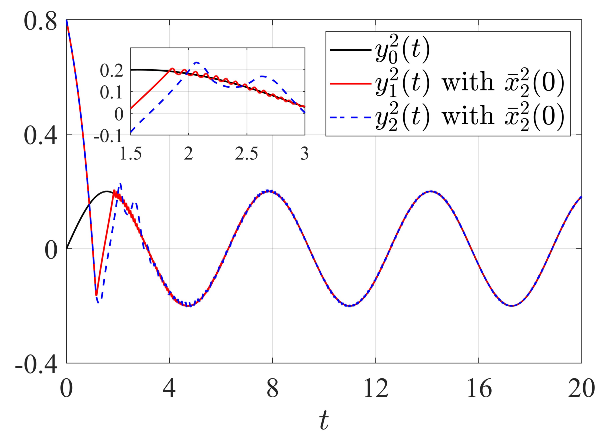


**Figure B4** Reference signal $y_0^2(t)$ and output trajectories.

Next, we provide comparisons with the controller in [11] to validate that the proposed control method's robustness against both the actuator faults and external disturbances. Consider the following perturbed pendulum system:

$$\begin{cases} \dot{x}_1(t) = x_2(t) + d_1(t), \\ \dot{x}_2(t) = -\frac{g\sin(x_1(t))}{l} - \frac{kx_2(t)}{m} + \frac{1}{ml^2}u(t) + d_2(t), \end{cases} \tag{B2}$$

where the dynamics originates from a nonlinear pendulum model $ml^2\ddot{q}(t) + mgl\sin(q(t)) + kl^2\dot{q}(t) = u(t)$ with $d_i(t), i = 1, 2$ representing external disturbances. They are set as $d_1(t) = 0.5\cos(2t)$ and $d_2(t) = 2\sin(t)$. Let reference signal $y_0^2(t) = 0.2\sin(t)$ and initial value $\bar{\boldsymbol{x}}_2^2(0) = [0.8, -1]^\top$. For clarity, the controller in [11] is denoted as $v''(t)$. In order to ensure precision and accuracy in simulations, the prescribed performance functions are set as $\rho_1^*(t) = (\frac{\pi}{2} - 0.05)e^{-0.5t} + 0.05$ and $\rho_2^*(t) = (\frac{\pi}{2} - 0.5)e^{-0.5t} + 0.5$. The controller parameters for the proposed control signal $v(t)$ in Eq. (A12) are set as $\bar{d}_1 = 0.01$, $\varrho_2 = 20$, $\varrho_2' = 0.01$, $\lambda_i = 1$, $\tau_i = 0.001$, $r_i = 1$, $\bar{r}_i = 10$, $\bar{h}_{ij} = 1$, $\bar{h}_{i3}(0) = 0$, where $i = 1, 2$, $j = 1, 2, 4$. Those for $v''(t)$ are set the same as that in [11]. To demonstrate the effect of an actuator fault, we add an actuator fault to both control signals i.e., $u(t) = 0.2v(t)$, $u''(t) = 0.2v''(t)$. Figures. B3-B4 present the simulation results.

Figure B3 compares the tracking performance of system (B2) under the proposed controller $v(t)$ and the existing approach $v''(t)$ from [11], evaluated through the tracking errors $\arctan(e(t))$ and $\arctan(e^{**}(t))$. While the benchmark method $v''(t)$ only achieves uniformly bounded error without convergence, our proposed $v(t)$ drives the tracking error to zero in finite time while preserving prescribed performance constraints (red solid line).

Figure B4 displays the reference signal $y_0^2(t)$ alongside the corresponding output trajectories under both control schemes. The output $y_1^2(t)$ (red solid line) generated by $v(t)$ and $y_2^2(t)$ (blue dashed line) produced by $v''(t)$ clearly demonstrate the improved transient performance of our method. Notably, the proposed controller exhibits faster convergence to the reference signal, confirming its theoretical soundness and practical superiority over conventional methods.

In summary, the proposed controller $v(t)$ in Eq. (A12) achieves finite-time exact tracking of reference signals in the presence of actuator faults, component faults, and external disturbances. Its superior performance is demonstrated through faster convergence and lower overshoot compared to existing methods.

**References**


1 Bechlioulis C P, Rovithakis G A. Adaptive control with guaranteed transient and steady state tracking error bounds for strict feedback systems. Automatica, 2009, 45: 532–538
2 Mao B, Wu X Q, Fan Z Y, et al. Performance-guaranteed finite-time tracking of strict-feedback systems with unknown control directions: A novel switching mechanism. IEEE Trans Autom Control, 2025, 70: 4061–4068
3 Zhang J X, Yang G H. Prescribed performance fault-tolerant control of uncertain nonlinear systems with unknown control directions. IEEE Trans Autom Control, 2017, 62: 6529–6535
4 Zhao K, Song Y D, Chen C L P, et al. Adaptive asymptotic tracking with global performance for nonlinear systems with unknown control directions. IEEE Trans Autom Control, 2022, 67: 1566–1573
5 Mao B, Fan Z Y, Wu X Q, et al. Design of asymmetric Lyapunov functions for global stability in dynamic surface control. Automatica, 2025, 182: 112544
6 Abdelhamid B, Mohamed C, Najib E. Indirect adaptive fuzzy fault-tolerant tracking control for mimo nonlinear systems with actuator and sensor failures. ISA Trans, 2018, 79: 45–61
7 Abdelhamid B, Mohamed C. Adaptive fuzzy fault-tolerant control using nussbaum-type function with state-dependent actuator failures. Neural Comput Appl, 2021, 33: 191–208
8 Abdelhamid B, Mohamed C. Robust fuzzy adaptive fault-tolerant control for a class of second-order nonlinear systems. Int J Adapt Control Signal Process, 2025, 39: 15–30
9 Chen W, Ge S S, Wu J, et al. Globally stable adaptive backstepping neural network control for uncertain strict-feedback systems with tracking accuracy known a priori. IEEE Trans Neural Netw Learn Syst, 2015, 26: 1842–1854
10 Niu B, Zhao J. Barrier Lyapunov functions for the output tracking control of constrained nonlinear switched systems. Syst Control Lett, 2013, 62: 963–971
11 Mao B, Wu X Q, Fan Z Y, et al. Performance-guaranteed finite-time tracking for uncertain strict-feedback nonlinear systems. IEEE Trans Circuits Syst II, 2024, 71: 375–379
12 Sontag E D. Mathematical control theory: Deterministic finite dimensional systems. 1998
13 Abdelhamid B, Mohamed C. General fuzzy adaptive fault-tolerant control based on nussbaum-type function with additive and multiplicative sensor and state-dependent actuator faults. Fuzzy Sets Syst, 2023, 468: 108616
14 Guo G, Zhang C L. Adaptive fault-tolerant control with global prescribed performance of strict-feedback systems. IEEE Trans Syst Man Cybern Syst, 2024, 54: 4832–4840
15 Kumar N, Chaudhary K S. Position tracking control of nonholonomic mobile robots via $H_\infty$-based adaptive fractional-order sliding mode controller. Math Model Control, 2025, 5: 121–130
16 Yuan R, An Z C, Shao S Y, et al. Dynamic event-triggered fault-tolerant cooperative resilient tracking control with prescribed performance for UAVs. Sci China Inf Sci, 2024, 67: 180205
17 Zheng Y, Wu X Q, Fan Z Y, et al. An improved topology identification method of complex dynamical networks. IEEE Trans Cybern, 2025, 55: 2165–2173
18 Zheng H W, Tian Y J. Exponential stability of time-delay systems with highly nonlinear impulses involving delays. Math Model Control, 2025, 5: 103–120